RESTORATION OF IMAGES CORRUPTED BY MULTIPLICATIVE NOISE IN THE NONSUBSAMPLED CONTOURLET DOMAIN

Fabrizio Argenti, Tiziano Bianchi, Giovanni Martucci di Scarfizzi, and Luciano Alparone

Università di Firenze
Dipartimento Elettronica e Telecomunicazioni
Via S. Marta 3, 50139, Firenze - Italy

ABSTRACT

The nonsubsampled contourlet transform (NSCT) is a powerful and versatile tool that allows a multiresolution and directional representation to be achieved. In this paper, we propose an extension of two despeckling algorithms, proposed to restore SAR images and based on the undecimated separable wavelet transform, to work into the NSCT domain. The signal is modeled as affected by a multiplicative noise. The noise–free NSCT coefficients are estimated from the observed ones according to either the *maximum–a–posteriori* (MAP) or the *linear minimum mean square error* (LMMSE) criterion. The results show that the proposed restoration algorithms highly benefit from the fact of working into a multiresolution and multidirectional domain.

Index Terms— Multiplicative noise, image denoising, nonsubsampled contourlet transform, MMSE filter, MAP filter

1. INTRODUCTION

The Contourlet Transform, both in its decimated [1] and in its nonsubsampled [2] version, is a powerful and versatile tool that allows *sparse* representation of 2–D signals to be achieved.

In this paper, we extend two despeckling algorithms [3, 4], proposed to restore SAR images and based on the undecimated separable wavelet transform, to work into the nonsubsampled contourlet domain. We will consider the following model for images corrupted by multiplicative noise

$$\begin{aligned} g(\mathbf{n}) &= f(\mathbf{n}) \cdot u(\mathbf{n}) = f(\mathbf{n}) + f(\mathbf{n}) \cdot [u(\mathbf{n}) - 1] \\ &= f(\mathbf{n}) + f(\mathbf{n}) \cdot u'(\mathbf{n}) = f(\mathbf{n}) + v(\mathbf{n}), \end{aligned} \tag{1}$$

where $\mathbf{n} = (n_1, n_2)$ is the pixel location, $g(\mathbf{n})$ and $f(\mathbf{n})$ represent the observed and noise–free images, respectively, whereas u represents the fading variable, modelled as a random, stationary, uncorrelated process, independent of f and with mean $E[u(\mathbf{n})] = 1$. The random process $u'(\mathbf{n}) \triangleq u(\mathbf{n}) - 1$ is zero–mean, with variance σ_u^2. The term $v(\mathbf{n}) = f(\mathbf{n}) \cdot u'(\mathbf{n})$ is a zero–mean *signal–dependent* noise term, proportional to the noise–free image $f(\mathbf{n})$.

The noise–free coefficients of the NSCT applied to the image are estimated from the observed ones according to either the *maximum–a–posteriori* (MAP) or the *linear minimum mean square error* (LMMSE) criterion. These algorithms rely on the definition of the equivalent filters that produce the NSCT coefficients of each subband and are based on estimating their moments up to the fourth order. The extension of the restoration algorithms into the NSCT domain, however, is not trivial since several implementation issues must be taken into consideration.

2. THE NONSUBSAMPLED CONTOURLET TRANSFORM

The NSCT can be seen as a combination of a nonsubsampled pyramid (NSP) and a nonsubsampled directional filterbank (NSDFB).

The NSP yields to the contourlet transform the *multiscale*, or *multiresolution*, property. This is achieved by lowpass and highpass filtering the original image. Let $A(\mathbf{z})$ and $B(\mathbf{z})$ be the lowpass and highpass filters resulting from the design. A multilevel representation is obtained by iterating the process, that is applying the lowpass-highpass decomposition to the *coarse* signal, until a desired degree of the coarseness is obtained. At each decomposition level, upsampled versions of $A(\mathbf{z})$ and $B(\mathbf{z})$ are used. The jth level subbands are achieved by using the equivalent filters $A_{j,eq}(\mathbf{z}) = \prod_{m=0}^{j-1} A\left(\mathbf{z}^{2^m \cdot \mathbf{I_2}}\right)$ and $B_{j,eq}(\mathbf{z}) = A_{j-1,eq}(\mathbf{z}) B\left(\mathbf{z}^{2^{(j-1)} \cdot \mathbf{I_2}}\right)$, where $\mathbf{I_2}$ identifies the 2×2 identity matrix. At the end of the procedure, the original input signal is expanded into several detail images (bandpass signals) plus the final coarse (lowpass) signal. The redundancy is $J + 1$, where J is the depth of the decomposition tree.

The NSDFB yields to the contourlet transform the *multidirection* property. The fundamental block for directional filterbank (DFB) construction is the two–channel quincunx filter bank (QFB), characterized by *hour-glass* and *fan* shaped filters, denoted as $U_0(z)$ and $U_1(z)$, and by subsampling and upsampling matrices. DFBs are obtained by cascading the output of the QFB with *quadrant* and with *parallelogram* shaped filters, thus obtaining a *wedge* shaped tiling of the bidimensional frequency plane. Upsampled versions of the filters $U_0(z)$ and $U_1(z)$ are used to implement the quadrant and parallelogram filters (see [1] for the details). The important result is that each channel of a DFB can be seen as an equivalent bidimensional filter followed by a final equivalent downsampling matrix. Consider, for example, an eight-subbands DFB. The transfer functions of the equivalent filters relative to the kth directional subband, $k = 0, 1, \ldots, 7$, can be expressed as

$$U_{k,eq}^{(8)}(\mathbf{z}) = U_p(\mathbf{z}) U_q(\mathbf{z}^{\mathbf{Q}_r}) U_s(\mathbf{z}^{2\mathbf{R}_i}), \tag{2}$$

where the indexes p, q, r, s can be either 0 or 1, $0 \leq i \leq 3$ and $\mathbf{Q}_r$ and $\mathbf{R}_i$ are appropriate downsampling matrices. For the proper selection of these indexes, depending on the index k, and the expressions of $\mathbf{Q}_r$ and $\mathbf{R}_i$ the reader can refer to [5]. The NSDFB is achieved by simply dropping the final equivalent downsampling matrix $\mathbf{M}_{k,eq}$, whose expression can be found in [5].

The nonsubsampled contourlet transform (NSCT) is achieved by first processing the input signal with a J-level NSP and then by decomposing the bandpass signals by means of a NSDFB. The number of directional channels can be different from one level to another: 2^{l_j} directional output channels are realized at the jth multiresolution level, with l_j an integer. Considering the definitions given above, the equivalent filters of a NSCT can be expressed as:

$$H_{J,eq}^{(\mathrm{low})}(\mathbf{z}) = A_{J,eq}(\mathbf{z}), \tag{3}$$

$$H_{j,k,eq}(\mathbf{z}) = B_{j,eq}(\mathbf{z}) \cdot U_{k,eq}^{(2^{l_j})}(\mathbf{z}), \tag{4}$$

where $1 \leq j \leq J$, $0 \leq k < 2^{l_j}$.

3. RESTORATION ALGORITHMS IN THE NSCT DOMAIN

In this section, the restoration algorithms proposed for images affected by a multiplicative noise will be described. The methods are extensions to the NSCT domain of the MAP and LMMSE estimators proposed for SAR images in [3] and [4].

In the following, we will assume that independent estimators are used for each subband. The NSCT equivalent filter $H_{j,k,eq}(\mathbf{z})$ and its impulse response will be simply denoted as $H(\mathbf{z})$ and $h(\mathbf{n})$, respectively. Hence, the NSCT coefficients of the signal x are defined by $W_x(\mathbf{n}) = \sum_{\mathbf{k}} h(\mathbf{k})x(\mathbf{n}-\mathbf{k})$. Applying the transform operator to the signal model in (1), thanks to the linearity of the NSCT, yields

$$W_g(\mathbf{n}) = W_f(\mathbf{n}) + W_v(\mathbf{n}). \tag{5}$$

The MAP estimator is obtained by maximizing the *a posteriori* probability density function of the noise-free NSCT coefficients ($W_f(\mathbf{n})$) conditional to the observed NSCT coefficients ($W_g(\mathbf{n})$), that, according to the proposed model, is equivalent to maximizing $p_{W_V|W_F}(W_g - W_f|W_f)p_{W_F}(W_f)$ [3]. As in [3], we will conjecture that the coefficients in the transform domain obey to a generalized Gaussian distribution (GGD) whose parameters locally vary. The GGD depends on its variance and on a shape parameter. Both parameters can be estimated pixelwise by relying on the second and fourth-order moments of the variables of interest [3].

As to the GGD's of interest, they are related to the non observable variables W_v and W_f, whose moments, however, can be estimated by using the moments of the observable variables g and W_g [3]. By using derivations similar to those presented in [3], we can demonstrate that the expressions of the second and fouth moments of W_v and W_f, defined in the NSCT domain, are given by

$$E\left[W_v^2(\mathbf{n})\right] = \frac{\mu_{u'}^{[2]}}{\mu_u^{[2]}} \sum_{\mathbf{i}} h^2(\mathbf{i}) E\left[g^2(\mathbf{n}-\mathbf{i})\right] \tag{6}$$

$$\begin{aligned} E\left[W_v^4(\mathbf{n})\right] \approx & \frac{\mu_{u'}^{[4]}}{1+6\sigma_{u'}^2+4\mu_{u'}^{[3]}+\mu_{u'}^{[4]}} \sum_{\mathbf{i}} h^4(\mathbf{i}) E\left[g^4(\mathbf{n}-\mathbf{i})\right] \\ & + 3\left(E\left[W_v^2(\mathbf{n})\right]\right)^2 \\ & - 3\left(\frac{\sigma_{u'}^2}{1+\sigma_{u'}^2}\right)^2 \sum_{\mathbf{i}} h^4(\mathbf{i}) \left(E\left[g^2(\mathbf{n}-\mathbf{i})\right]\right)^2 \end{aligned} \tag{7}$$

$$E\left[W_f^2(\mathbf{n})\right] = E\left[W_g^2(\mathbf{n})\right] - E\left[W_v^2(\mathbf{n})\right] \tag{8}$$

$$E\left[W_f^4(\mathbf{n})\right] \approx E\left[W_g^4(\mathbf{n})\right] - E\left[W_v^4(\mathbf{n})\right] \tag{9}$$

where $\mu_x^{[k]}$ denotes the kth moment of the random variable x,

The MAP estimator is finally defined as

$$\widehat{W}_f(\mathbf{n}) = \underset{W_f(\mathbf{n})}{\operatorname{argmax}}\, \phi(W_f(\mathbf{n})) \tag{10}$$

where $\phi(W_f(\mathbf{n}))$ is a log-MAP functional depending on the above four moments and whose expression can be found in [3].

The expression of the LMMSE estimator in the case of restoration into the separable undecimated wavelet domain was presented in [4]. It involves moments of the variables that have been previously considered up to the second order. The LMMSE criterion can be reformulated into the NSCT domain in a straightforward way as follows:

$$\widehat{W}_f(\mathbf{n}) = E\left[W_g(\mathbf{n})\right] + \frac{\sigma_{W_f}^2(\mathbf{n})}{\sigma_{W_g}^2(\mathbf{n})}(W_g(\mathbf{n}) - E\left[W_g(\mathbf{n})\right]). \tag{11}$$

4. IMPLEMENTATION ISSUES

4.1. Directional subbands at the first multiresolution level

Due to the tree-structure of the NSDFB, the directional subbands are implemented by means of equivalent filters which suffer from aliasing at the lower and upper frequencies [2, 6]. In [2], it is suggested to interpolate the NSDFB when filtering the coarser levels of the NSP. Unfortunately, this solution is not effective when dealing with the first multiresolution level [6], since the passband of the NSP comprehends the frequencies from $\pm\pi/2$ to $\pm\pi$, which are affected by the aliasing of the NSDFB at the higher frequencies.

The proposed solution consists of interpolating the first level of the NSP by a factor two before applying the directional filterbank. This operation shrinks the passband of the NSP between $\pm\pi/4$ and $\pm\pi/2$, so that the interpolated NSP coefficients are not affected by the area of the NSDFB frequency response in which aliasing occurs. In order to maintain the perfect reconstruction, a very simple solution is obtained by using as interpolating filter on both the rows and the columns an half-band filter. As to the reconstruction, it suffices to decimate by a factor two the output of the synthesis NSDFB before applying the synthesis NSP.

The estimation procedure of the moments of the first level is slightly modified in order to cope with the interpolation. Denoting as $W_{G,1,k}(\mathbf{z})$ the output of the kth subband at the first multiresolution level after interpolation, we have

$$\begin{aligned} W_{G,1,k}(\mathbf{z}) =& U_{k,eq}^{(2^{l_1})}(\mathbf{z}) S(\mathbf{z}) B_{1,eq}(\mathbf{z}^{2\mathbf{I_2}}) G(\mathbf{z}^{2\mathbf{I_2}}) \\ =& \tilde{H}_{1,k,eq}(\mathbf{z}) G(\mathbf{z}^{2\mathbf{I_2}}) \end{aligned} \tag{12}$$

where $S(\mathbf{z})$ indicates the interpolating filter and $G(\mathbf{z})$ is the $\mathcal{Z}$-transform of $g(\mathbf{n})$. Hence, the moments can be estimated by filtering an interpolated version of g with the equivalent filters $\tilde{H}_{1,k,eq}(\mathbf{z})$.

4.2. Estimation of moments by using local averages

The estimation of the moments of W_f and W_v is based on the knowledge of the moments of the observable quantities g and W_g. In the implementation of the filter, these moments will be approximated by local averages, assuming that the underlying signal is locally stationary and ergodic. The moments of g will be estimated as

$$E[g^\gamma(\mathbf{n})] \approx \overline{g^\gamma(\mathbf{n})} = \sum_{\mathbf{i} \in \mathcal{S}_W} p(\mathbf{i}) g^\gamma(\mathbf{n}+\mathbf{i}), \tag{13}$$

where $\mathcal{S}_W$ indicates the support of the averaging window, $\gamma = 2, 4$, and $p(\mathbf{i})$ are suitable normalized weights. Usually, $\mathcal{S}_W$ is a square $N \times N$ (N odd) window centered at $\mathbf{i} = (0, 0)$, and the coefficients $p(\mathbf{i})$ are taken from a Gaussian window.

As to the moments of W_g, it is observed that the undecimated contourlet coefficients are locally correlated, with a correlation pattern depending on the equivalent downsampling matrix $\mathbf{M}_{k,eq}$. In order to apply the locally stationary and ergodic assumption, the support of the signal used to estimate the local averages should depend on the equivalent downsampling matrix, that is only samples belonging to the lattice generated by $\mathbf{M}_{k,eq}$ should be considered. Hence, the estimator of the moments of W_g can be expressed as

$$E[W_g^{\gamma}(\mathbf{n})] \approx \overline{W_g^{\gamma}(\mathbf{n})} = \sum_{\mathbf{i} \in \mathcal{S}_W} p(\mathbf{i}) W_g^{\gamma}(\mathbf{n} + \mathbf{M}_{k,eq}\mathbf{i}). \qquad (14)$$

4.3. Border extensions

Perfect reconstruction at the borders is obtained by means of either periodic or symmetric extensions for the NSP, whereas only periodic extension can be used for the NSDFB when implemented with the *à trous* algorithm. Conversely, when the equivalent filters are used to estimate the signal moments only one of the two types of extension at the borders can be implemented. As a result, we may have different types of extensions at the borders for the NSCT coefficients and for the estimates of the moments. The following solutions are proposed:

symmetric solution: use the equivalent filters also to compute the NSCT coefficients (NSCT-S). In this case a symmetric extension can be used for both NSCT and moment computations. The main advantage is that both NSCT coefficients and moment estimates are derived relying on the same filters. The drawback is that filtering with an equivalent and not separable filter can be very expensive;

mixed solution: use the equivalent filters with symmentric extension for the moments and *à trous* algorithm (NSP with symmetric, NSDFB with periodic extension) to compute the NSCT coefficients (NSCT-M). In this case we maintain the advantage of an *à trous* implementation. However, the moment estimates obtained through the equivalent filters may not reflect the properties of the NSCT coefficients near the borders;

periodic solution: use the *à trous* algorithm with periodic extension for both the NSP and the NSDFB, and the equivalent filters with periodic extension for moment estimation. In this case, both *à trous* implementation and equivalent filters yield the same behavior. A possible drawback is that periodic extension can lead to some artifacts near the borders, due to the introduction of discontinuities.

4.4. Equivalent filter truncation

The estimation of the moments of W_f and W_v requires to filter some moments of g with the equivalent filters raised to the second and the fourth power. In this case no *à trous* algorithm can be used, since the prototype filters yielding both $h^2(\mathbf{n})$ and $h^4(\mathbf{n})$ are not defined. Moreover, due to their usual large dimensions, computations using the non-separable equivalent filters may be very cumbersome.

As a practical solution, we propose to truncate the equivalent filters when they are used to estimate the moments. The new dimension of the filters are chosen so that 99% of the filter energy is retained. It is observed that such a strategy permits a reduction up to $1/10$ in both filter dimensions, with a complexity reduction up to $1/100$. Note that the approximation on the moments estimates can be assumed as negligible.

5. EXPERIMENTAL RESULTS

The performance of the proposed methods has been assessed by means of images affected by synthetically generated multiplicative noise. Two test images were used: “Barbara” and “Lena”. We have assumed that the fading variable u is distributed as a $\Gamma(L, L)$ function, i.e., $p_U(u) = \frac{L^L}{\Gamma(L)} u^{L-1} e^{-uL}$. This assumption is consistent

Table 1. PSNR values obtained with the different filters.

MAP estimator on “Barbara”					
L	Raw	UWT	NSCT-S	NSCT-ST	NSCT-MT
1	12.31	22.84	**23.30**	23.20	23.17
4	17.99	26.41	**26.99**	26.90	26.90
16	23.99	30.36	**30.81**	30.75	30.80
MAP estimator on “Lena”					
L	Raw	UWT	NSCT-S	NSCT-ST	NSCT-MT
1	12.09	26.21	**26.54**	26.45	26.37
4	17.78	29.59	**29.93**	29.78	29.78
16	23.74	33.06	**33.39**	33.26	33.24
LMMSE estimator on “Barbara”					
L	Raw	UWT	NSCT-S	NSCT-ST	NSCT-MT
1	12.31	22.46	**23.06**	22.91	22.88
4	17.99	26.05	**26.78**	26.67	26.67
16	23.99	30.20	**30.78**	30.71	30.74
LMMSE estimator on “Lena”					
L	Raw	UWT	NSCT-S	NSCT-ST	NSCT-MT
1	12.09	24.23	**25.14**	24.84	24.77
4	17.78	28.27	**29.18**	28.94	28.90
16	23.74	32.42	**33.07**	32.93	32.90

Table 2. Approximate computation times (in seconds) for the proposed algorithms.

	UWT	NSCT-S	NSCT-ST	NSCT-MT
MAP	$2.5\ 10^2$	$1.7\ 10^4$	$6.5\ 10^3$	$2.0\ 10^3$
LMMSE	25	$9.5\ 10^3$	$5.5\ 10^3$	$1.2\ 10^3$

with the “intensity” signal model of coherent imaging systems, like Synthetic Aperture Radar (SAR), processed with L-looks averaging [7]. Note that the only knowledge we need about the fading variable consists of its moments up to the fourth order.

The images have been processed in the NSCT domain, both with the MAP and the LMMSE estimator. The NSCT domain consists of 4 multiresolution levels. The number of directional subbands in each multiresolution level, from finer to coarser, is 8, 8, 4, 4. The results are compared with those obtained with the undecimated wavelet transform (UWT) [3, 4] by using the same number of multiresolution levels.

The NSCT subbands were obtained by using the “maxflat” and the “dmaxflat7” filters [2], for the NSP and the NSDFB, whereas 9/7-taps biorthogonal filters were used for the UWT. As to the NSCT implementation, we consider the following filters: NSCT-S (symmetric solution), NSCT-ST (symmetric solution with truncation), NSCT-MT (mixed solution with truncation). The implementation using periodic extensions always achieved a worse result than NSCT-S and NSCT-M, therefore its performance has not been reported.

The results for both MAP and LMMSE estimators are reported in Table 1. Several noise levels, indicated with the number of looks L, have been used.

As to the computational complexity, the times needed to run the above referred algorithms are shown in Table 2. A Matlab® implementation running on a laptop equipped with a Centrino® 1.73 GHz processor has been used.

From these tables it can be observed that using truncation and the *à trous* algorithm yields in general only a slight degradation of the performance in terms of PSNR whereas they strongly reduce the computational burden. From the comparison between the MAP and

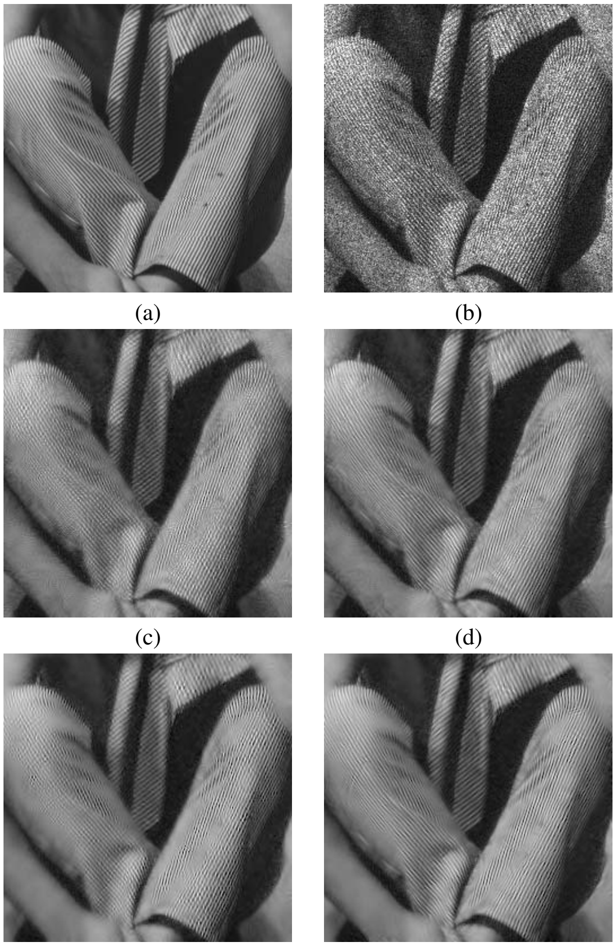

(a) (b) (c) (d) (e) (f)

Fig. 1. A detail of the restored images "Barbara": original (a), noise-corrupted ($L = 4$) (b), LMMSE estimator in the UWT domain (c), LMMSE estimator in the NSCT domain (d), MAP estimator in the UWT domain (e), MAP estimator in the NSCT domain (f).

the LMMSE estimator it can be understood that the former is superior to the latter, according to the fact that LMMSE estimator is optimum only in the case of Gaussian signals, whereas tha MAP estimator exploits more information we have about the signal. Finally, from the comparison between the results obtained in the UWT and in the NSCT domains it is apparent that the NSCT outperforms the UWT. This fact confirms that using a representation able to discriminate directional features yields a significant improvement in the application of denoising images affected by multiplicative noise.

These considerations about the performance of the different representations and estimators are confirmed by an inspection of some visual results. In Fig. 1 the original and noisy versions ($L = 4$) of a particular of "Barbara" and the restored images obtained by using the LMMSE and MAP estimators in the UWT and in the NSCT domain are presented.

Finally, the effectiveness of the solution proposed for the first multiresolution level can be verified in Fig. 2. As can be seen, the interpolation of the first level greatly reduces the aliasing effects, which are visible in the high frequency directional artifacts.

(a) (b)

Fig. 2. A detail of the restored images "Lena" using MAP estimator in the NSCT domain: first multiresolution level is not interpolated (a), first multiresolution level is interpolated by a factor two (b).

6. CONCLUDING REMARKS

We have investigated the restoration of images corrupted by multiplicative noise in the nonsubsampled contourlet domain. Both the LMMSE and the MAP filters, previously proposed in the undecimated wavelet domain, were adapted for working with the directional transform. Several issues were tackled with, including the problem of directional aliasing at high frequencies, the impossibility of defining an exactly equivalent filter due to the extension at the borders, and the growth of complexity due to non separable filtering. The results show that the filters defined in the NSCT domain outperform the previous filters. Moreover, the proposed solutions show that the complexity of filtering in the NSCT domain can be noticeably reduced at the cost of a very small performance loss.

7. REFERENCES

[1] M. N. Do and M. Vetterli. The contourlet transform: An efficient directional multiresolution image representation. *IEEE Trans. Image Process.*, 14(12):2091–2106, Dec. 2005.

[2] A. L. da Cunha, J. Zhou, and M. N. Do. The nosubsampled contourlet transform: Theory, design and applications. *IEEE Trans. Image Process.*, 15(10):3089–3101, Oct. 2006.

[3] F. Argenti, T. Bianchi, and L. Alparone. Multiresolution MAP despeckling of SAR images based on locally adaptive generalized Gaussian pdf modeling. *IEEE Trans. Image Processing*, 15(11):3385–3399, Nov. 2006.

[4] F. Argenti and L. Alparone. Speckle removal from SAR images in the undecimated wavelet domain. *IEEE Trans. Geosci. Remote Sensing*, 40(11):2363–2374, Nov. 2002.

[5] M. N. Do. *Directional multiresolution image representations*. PhD thesis, School Comput. Commun. Sci., Swiss Fed. Inst. Technol., Lausanne, Switzerland, 2001.

[6] Y. Lu and M. N. Do. A new contourlet transform with sharp frequency localization. In *Proc. IEEE Int. Conf. Image Process. (ICIP)*, pages 1629–1632, Atlanta, GA, Oct. 2006.

[7] C. Oliver and S. Quegan. *Understanding Synthetic Aperture Radar Images*. Artech House, Boston, MA, 1998.